AN AUDIO FREQUENCY FILTER APPLICATION OF MICROMACHINED THERMALLY-ISOLATED DIAPHRAGM STRUCTURES

Kwang-Hyun Lee, Hee-Jin Byun, Hyung-Kew Lee, Il-Joo Cho, Jong-Uk Bu* and Euisik Yoon

Department of Electrical Engineering
Korea Advanced Institute of Science and Technology (KAIST)
373-1, Kusong-dong, Yusong-gu, Teajon, Korea
*LG Corporate Institute of Technology, Seoul, Korea
e-mail: khlee@iml.kaist.ac.kr

ABSTRACT

This paper reports a new application of micromachined thermally-isolated diaphragm structures for audio frequency filters. We have used a pair of electrothermal elements that consist of a heater and a temperature sensor integrated in the same dielectric diaphragm for a good thermal coupling. The filters using the fabricated electrothermal structures with driving circuitry have been tested. Measured responses of the filters show that a cut-off frequency can be electrically tuned ranging from 30Hz to 300Hz. Design parameters with respect to filter characteristics have been analyzed and design guidelines have been identified. The results have demonstrated the possibility that the thermally-isolated diaphragm structures can be used for audio frequency filter applications.

INTRODUCTION

Previously, the micromachined electrothermal structures were used for mass flow sensors, rms-dc converters, infrared sensors, etc. [1-4]. These applications take advantage of the structures such as low thermal conductance for effective temperature sensing and large thermal capacitance for low frequency filtering. Generally, micromachined structures can give these desirable characteristics implemented by IC compatible processes in a small size. In this paper, we have demonstrated the filter applications of the micromachined electrothermal structure in the audio frequency range with driving circuitry. In general, audio-band electrical filters have been designed using Gm-C or switched capacitor techniques. However, they have some drawbacks. Gm-C filters require large capacitors and low-gain transconductors while switched capacitor filters typically have high switching noise and aliasing effects. It has been reported that, by using the large effective time constant that can be obtained in temperature domain, the realization of audio frequency range filters becomes much easy and simple [5,6]. In the previous approaches the bulk silicon has been used as a thermal structure, to make the filter bulky, consume large power, and difficult to control thermal characteristics. We reports the filter application of the micromachined electrothermal structure which is ease to customize the thermal characteristics. In this paper, design factors and basic considerations for optimizing design parameters using the electrothermal structures will be presented. Test results of the fabricated electrothermal structures and filters demonstrated followed by the discussion of the audio frequency filter design using the micromachined electrothermal structures.

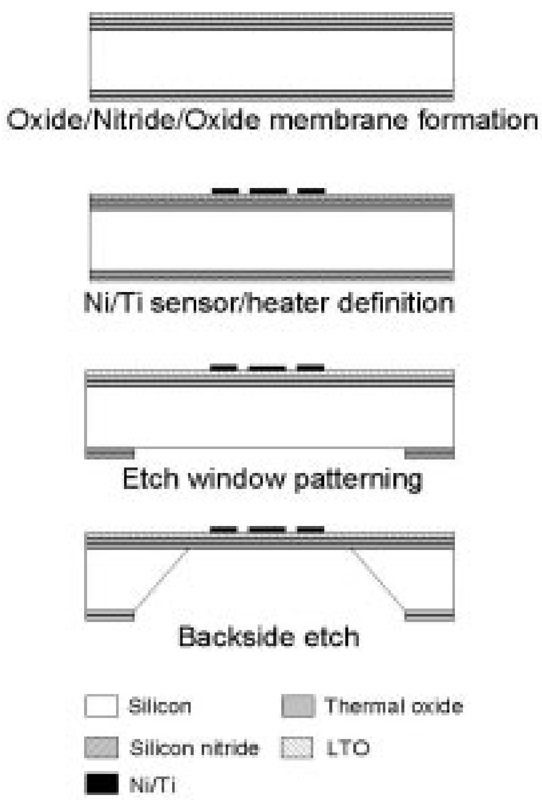

Figure 1: Fabrication Process Flow

FABRICATION PROCESS

Figure 1 shows the fabrication process flow of the electrothermal diaphragm structures. It consists of a thin diaphragm for thermal isolation and two metal resistors as a sensor and a heater. The membrane has been fabricated using a silicon oxide/silicon nitride/silicon oxide multi-layer. First, thermal silicon oxide is grown followed by the deposition of silicon nitride by LPCVD. Low temperature oxide (LTO) is deposited as the third layer of the membrane. The heater and sensor resistors are deposited and patterned by lift-off technique. We have used nickel for the metal resistors with titanium as an adhesion layer. Each layer has thicknesses of 400Å and 100Å, respectively. Temperature coefficient of resistance (TCR) of the metal resistor has been measured as 0.24%/K. Finally, etch window is defined in the backside followed by anisotropic silicon etch in 25% KOH at 85°C for 7 hours. The fabricated electrothermal structures are shown in Figure 2. Typically, they have a diaphragm size of 500μm × 500μm, sensor resistance of 3kΩ, heater resistance of 1.7kΩ, and thermal conductance of about 1.5×10^{-4}W/K, respectively.

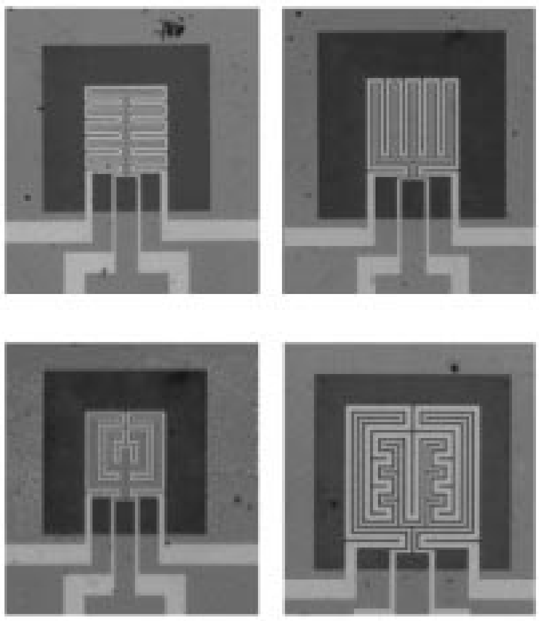

Figure 2: Microphotographs of the fabricated thermally-isolated diaphragm structures.

PRINCIPLE OF FILTER OPERATION

Figure 3 shows the principle of filter operation using the electrothermal structures. A sinusoidal signal superimposed with dc bias level is applied to the heating resistor and the temperature variation of the sensor resistor is converted into an electrical output signal. The temperature of the diaphragm cannot respond as fast as the variation of the input sinusoidal signal because of thermal mass; i.e., filtering out high frequency components. Figure 4 shows the typical thermal characteristics of the structure. It shows one-pole low-pass characteristics with a time constant of 9.8msec.

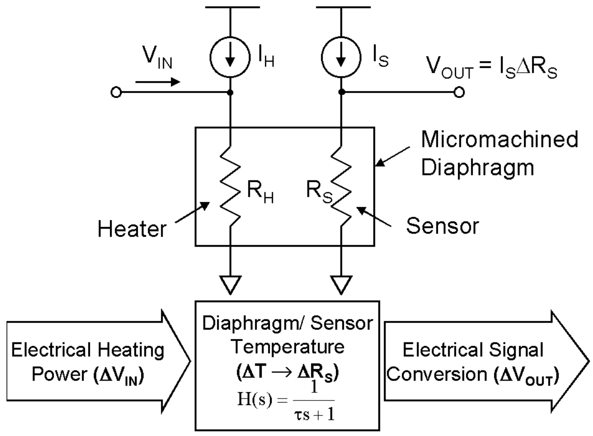

Figure 3: Principle of filter operation in the electrothermal structure

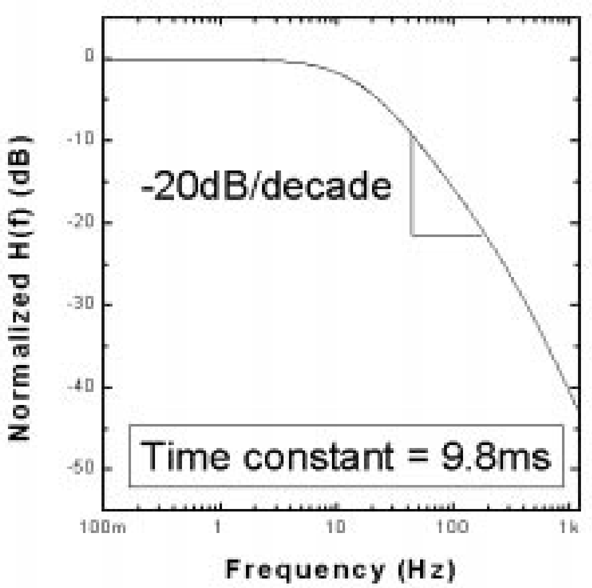

Figure 4: Typical measured thermal characteristics of the diaphragm structure

FILTER DESIGN

Analogically, the electrothermal structures with driving circuitry using transconductors can be viewed as an electrical Gm-C integrator. The temperature of diaphragm is varied according to applied electrical power. However, we cannot cool down the diaphragm by electrical manner. Therefore, quiescent bias power must be applied to the electrothermal structure through a heater in order to maintain the signal integrity in the thermal domain. For a given bias current, the quiescent temperature increase of the diaphragm is given by

$$\Delta T = \frac{I_S^2 R_S + I_H^2 R_H}{G_{th} - (I_S^2 R_S + I_H^2 R_H)\alpha} \quad (1)$$

where I_H and I_S are bias currents of a heater and a sensor, respectively, R_H and R_S are resistance values of a heater and a sensor, respectively, α is TCR of the sensor resistor, G_{th} and C_{th} are thermal conductance and thermal capacitance of the structure, respectively. Bias currents of the heating and sensing resistors must be determined from electromigration limit, power consumption requirement and temperature limit of the electrothermal structure.

Figure 5 shows schematic diagrams comparing a simple Gm-C integrator with an electrothermal integrator using the thermal structure. The ideal integrator should have a pole located at zero frequency. However, nonzero G_{th} of the electrothermal structure makes the integrator characteristics deviate from the ideal case. This non-zero pole location introduces distortions in the filter transfer characteristics.

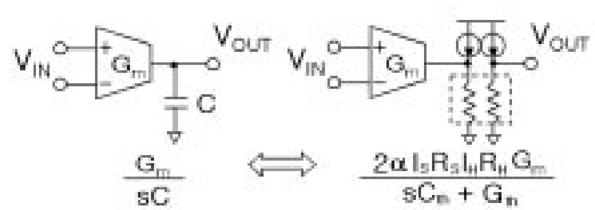

Figure 5: Analogy between electrical Gm-C integrator and electrothermal integrator

Let us take a look at the electrothermal filter characteristics in more detail. The input signal applied to the structure is converted to a temperature signal by resistive heating power. This power is proportional to the square of the applied input current; therefore, the electrothermal integrator has nonlinear transfer characteristics. If the power variation by a.c signal is relatively smaller than the quiescent power, the relationship between the input electrical signal and power conversion can be approximately linearized as follows

$$\delta\phi = 2 I_H R_H i_h = 2\phi_H / I_H \cdot i_h \quad (2)$$

where $\delta\phi$ is the a.c. power signal and ϕ_H is the bias power of the heating resistor. The second order harmonic distortion (HD_2) is given by

$$HD_2 = \frac{i_h}{4 I_H}. \quad (3)$$

The quantity $2I_H R_H$ or $2\phi_H/I_H$ can be viewed as a power conversion gain. If a high conversion gain is required, a large heating resistor or a smaller bias current can be used for a given bias condition.

If we use identical heating and sensing resistors ($R=R_H=R_S$) and the same bias current ($I_B=I_H=I_S$), the unity gain frequency of the integrator is given by

$$\omega_T = \frac{2\alpha I_B^2 R^2 g_m}{C_{th}}. \quad (4)$$

In the filter design, characteristic frequencies, such as cut-off frequency in low-pass filters and center frequency in band-pass filters should be near ω_T. The characteristic frequencies can be tuned by various parameters such as bias current, transconductance, resistance value, thermal capacitance and TCR. It would be desirable that tuning procedure can be performed by customizing electrical parameters rather than thermal ones. In addition, ω_T can be represented by other parameters as follows.

$$\omega_T = \frac{\alpha\phi_B R g_m}{C_{th}} = \frac{\alpha G_{th}\Delta T R g_m}{C_{th}} = \alpha\omega_P \Delta T R g_m \quad (5)$$

where ω_P is the pole of the electrothermal structure. These equations for the unity gain frequency give us additional understandings. As discussed previously, non-zero pole of the integrator results in the distortion in the transfer function. This distortion can be specified as a phase error given by

$$\varphi_{error} = 90^o - tan^{-1}\left(\frac{\omega_T}{\omega_P}\right) \quad (6)$$

where $\omega_P=G_{th}/C_{th}$. If $\omega_T \geq 100\omega_P$, the phase error will be less than 0.5°. For a given phase error, the minimum g_m can be determined by

$$g_{m\,min} = \frac{\omega_T}{\alpha\omega_P \Delta T R}. \quad (7)$$

This is the minimum value of g_m that should be used in the circuit to guarantee the given phase error specification. For example, assuming that $\omega_T=100\omega_P$, ΔT=30°C, R=5kΩ and α=0.2%K^{-1}, the required minimum g_m will be about 300mA/V.

One of the important aspects that should be considered in the electrothermal filter design is signal dynamic range. The maximum variation in the sensor output voltage must be large enough to meet the required dynamic range. Let the maximum variation of the sensor output voltage be v_{max}. The heater driving circuitry must provide the current that makes sensor voltage swing up to v_{max} at ω_T. Therefore,

$$2 I_B R i_{\max} = \omega_T C_{th} \delta T \quad (8)$$

$$v_{max} = \frac{2\alpha I_B^2 R^2 i_{max}}{\omega_T C_{th}} \quad (9)$$

Substituting (4) into (9) gives

$$i_{max} = g_{m\,max} v_{max} \,. \tag{10}$$

In the filter design, v_{max} must be large enough to meet the dynamic range requirement. Because i_{max} cannot exceed the bias current (I_B), g_m should have a upper limit. In addition, It should be noted that large i_{max} causes harmonic distortion. This g_m restriction is due to the quiescent bias operation of the electrothermal structure. From (3) and (10), the maximum g_m can be found as $4HD_2I_B/v_{max}$. If we express it using G_{th} and quiescent temperature ΔT instead of I_B, $g_{m\,max}$ is given by

$$g_{m\,max} = \frac{4HD_2}{v_{max}}\sqrt{\frac{G_{th}\Delta T}{2R}} \,. \tag{11}$$

From the minimum and maximum restrictions imposed on g_m, the tunable range of ω_T can be determined. The minimum tunable ω_T is given by the phase error and ω_P as follows

$$\omega_{T\,min} = \omega_P \, tan\left(90^o - \varphi_{error}\right). \tag{12}$$

By substituting (11) into (5), the maximum tunable ω_T is given by

$$\omega_{T\,max} = \alpha\omega_P \Delta T \frac{HD_2}{v_{max}}\sqrt{8G_{th}R\Delta T} \,. \tag{13}$$

Based on the previous discussions, electrothermal filter design procedure can be summarized as follows. From (10), it is desirable that g_m is maintained as small as possible for a large dynamic range and low power consumption. The minimum g_m value at a given phase error specification is given by (7). Next, I_B should be determined. I_B should be larger than i_{max} and be suitable for a given HD_2. It is highly desirable that differential circuits should be employed for canceling out even harmonic distortions. Also, I_B should not be larger than electromigration limit. Even if the electromigration limit is satisfied, the quiescent power, approximately given by $2I_B^2R$, should be carefully reviewed. The electrothermal structure should not cause thermal runaway or excess temperature rising at this bias of I_B. Note that the electrothermal structure should have C_{th} large enough to guarantee that $\omega_P << \omega_T$. Finally, all above requirements are met, ω_T can be tuned in the range given by (12) and (13).

EXPERIMENTS

The basic circuitry for electrically configurable filters is shown in Figure 6. This circuit is adapted from the Gm-C filter scheme. Differential circuit technique is employed to reduce the even harmonic distortion. The transfer function of the circuit is given by

$$H(s) = \frac{2\alpha A I_S I_H R_S R_H G_{m1}}{sC_{th} + (2\alpha A I_S I_H R_S R_H G_{m2} + G_{th})} \tag{14}$$

This circuit forms a first-order low-pass filter and is electrically tunable by properly adjusting transconductances (G_{m1}, G_{m2}), amplifier gain (A), or bias currents (I_H, I_S) as denoted in the equation. Shown in Figure 7 are measured responses of the filter when transconductance is varied to tune a cut-off frequency ranging from 30Hz to 300Hz with A=100.

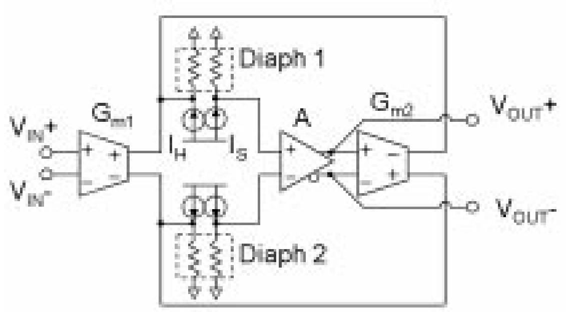

Figure 6: Schematic diagram of basic filter block.

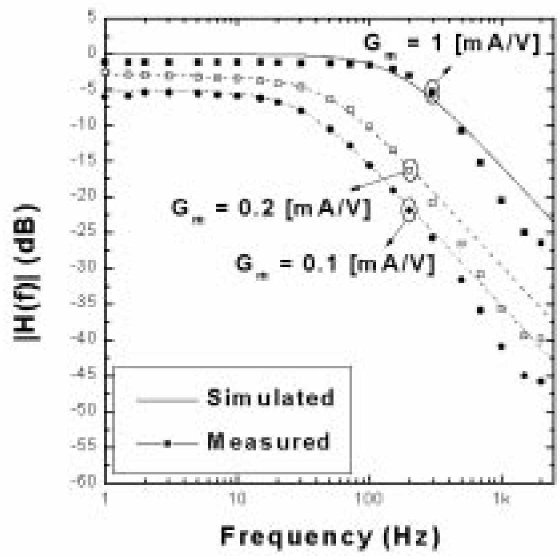

Figure 7: Frequency responses of the 1-st order low-pass filter.

The second-order filter characteristics has been tested using bi-quad connection of the basic blocks as shown in Figure 8. Figure 9 shows measured band-pass transfer characteristics. The center frequency of the BPFs can be tuned in the similar way up to 300Hz.

DISCUSSIONS

Figure 10 shows the minimum required thermal conductance for the electrothermal filter tuned to f_T where $f_T = \omega_T/2\pi$ This plot shows two possible materials

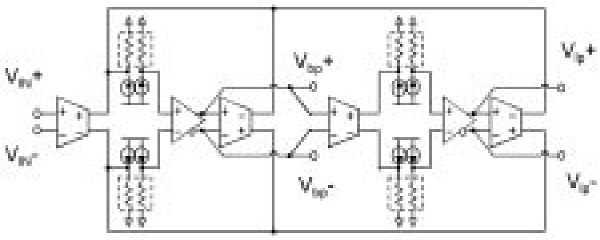

Figure 8: Schematic diagram of the 2nd-order filter.

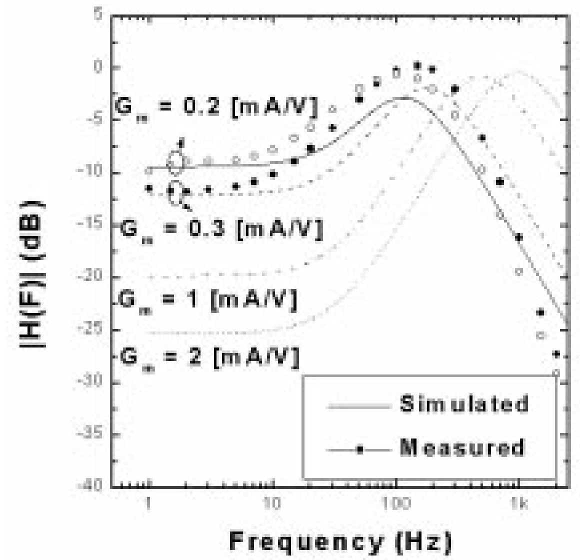

Figure 9: Frequency response of the 2nd order bandpass filter.

for heating and sensing resistors [4,7]. Titanium resistors have a typical TCR of about 0.2% while vanadium oxide resistors have that of about 2%. If f_T forms near at 100Hz, the pole of electrothermal structure, ω_T, should be below 6.3rad/s for <0.5° phase error. It is assumed that ΔT=20K and v_{max}=2mV for a dynamic range of 60dB with thermal noise at 10kHz bandwidth. As this plot shows, titanium resistors of ω_p=6.3rad/s is hard to be used to tune above 100Hz because of electromigration limit (a few mA) and excess power consumption (above 10mW). Figure 11 shows the simulated 2nd-order BPF transfer characteristics for the fabricated structure which has nickel/titanium resistors and the thermal characteristics with ω_p=70rad/s.

As shown in Figure 10 and 11, the electrothermal structure can be tuned up to about 300Hz with a bias current of 1mA. In this case, ω_T/ω_P is not sufficiently high enough to tune the whole audio frequencies. This is why Figure 7 shows seriously-degenerated transfer characteristics.

Electrothermal structures using a high TCR material (e.g. vanadium oxide) is expected to be more suitable elements for audio frequency filter design. This is mainly due to the high TCR value. Figure 12 shows the simulated BPF characteristics assuming that the TCR of the resistors in the electrothermal structure is 2%.

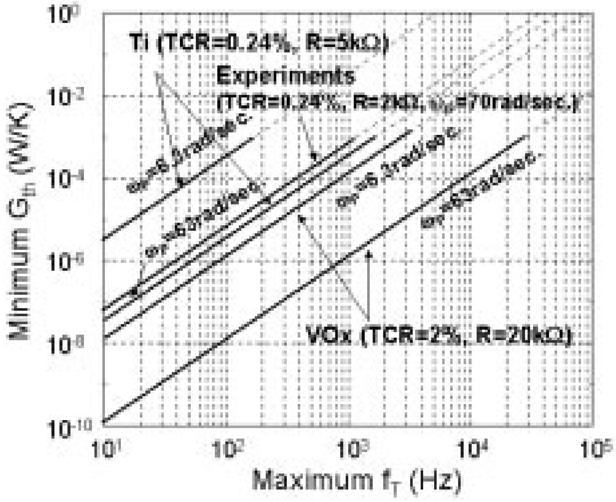

Figure 10: Minimum required thermal conductance(G_{th}) corresponding to f_T

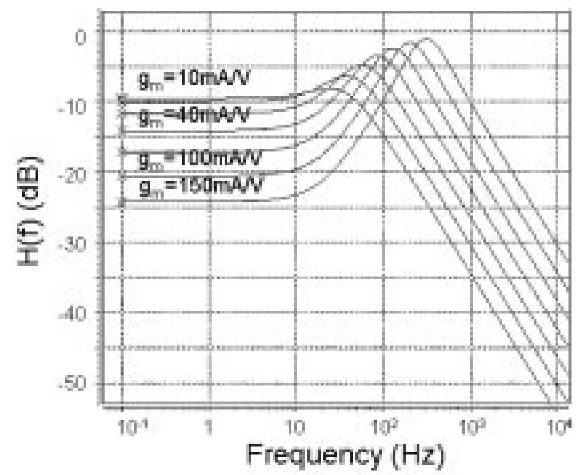

Figure 11: Simulated 2nd-order BPF transfer characteristics for the fabricated electrothermal structure

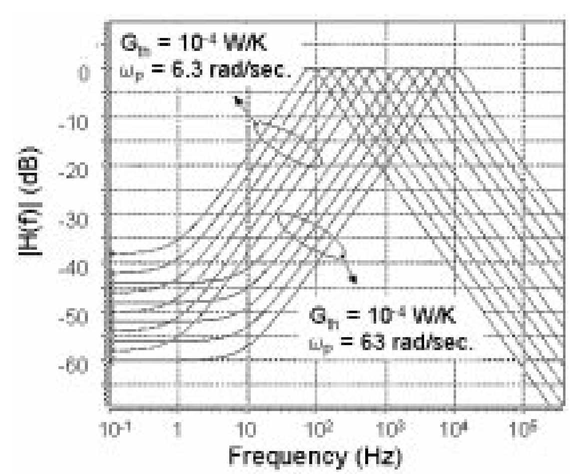

Figure 12: Simulated 2nd-order BPF characteristics using the material with a high TCR of 2%

For the frequency ranges from 100Hz to 1kHz and from 1kHz to 10kHz, two different diaphragms of ω_P=6.3rad/s and 63rad/s have been used for simulations, respectively. This is because it is more desirable to use the structure with a high ω_P for tuning the filter in the high frequency range to reduce power consumption. Simulation results show that about 2mW quiescent power is dissipated per each thermal structure. Transconductances have been tuned in the range of 10mA/V to 100mA/V in the entire audio frequency ranges.

CONCLUSIONS

We have demonstrated the electrothermal filter applications of the thermally-isolated diaphragm structures. Low-pass and band-pass electrothermal filters have been fabricated, tested and tuned from 30Hz to 300Hz. It has been suggested from the simulations that electrothermal filters can be realized in the audio frequency range (from 100Hz to 10kHz) when the materials with a TCR higher than 2%K^{-1} are used for the resistors in the thermal structure. These electrothermal filters can be applied to audio band filter applications such as implementation of basilar membrane models and loop filters in the automatic adaptation technique.

ACKNOWLEDGMENTS

This work has been partially supported by the G7 project from Ministry of Industry and Energy and Ministry of Science and Technology of Korea, and partially supported by Brain Science Research Center at KAIST.

REFERENCES

[1] E. Yoon and K. D. Wise, "An integrated mass flow sensor with on-chip CMOS interface circuitry," *IEEE Trans. Electron Devices*, pp.1376-1386, June 1992.

[2] E. Yoon and K. D. Wise, "A wideband monolithic rms-dc converter using micromachined diaphragm structures," *IEEE Trans. Electron Devices*, pp.1666-1668, Sep. 1994.

[3] P. E. Eriksson, J. Y. Andersson and G. Stemme, "Thermal characterization of surface-micromachined silicon nitride membranes for thermal infrared detectors," *IEEE J. Microelectromechanical Systems*, pp.55-61, March 1997.

[4] H. K. Lee, J. B. Yoon, E. Yoon, S. B. Ju, Y. J. Yong, W. Lee, and S. G. Kim, "A high fill-factor infrared bolometer using micromachined multilevel electrothermal structures," *IEEE Trans. Electron Devices*, pp.1489-1491, July 1999.

[5] P. R. Gray and D. J. Hamilton, "Analysis of electrothermal integrated circuits," *IEEE J. Solid-State Circuits*, pp. 8-14, Feb. 1971.

[6] W. J. Louw, D. J. Hamilton, and W. J. Kerwin, "Inductor-less, capacitor-less state-variable electrothermal filters," *IEEE J. Solid-State Circuits*, pp. 416-423, Aug. 1977.

[7] B. E. Cole, R. E. Higashi, and R. A. Wood, "Monolithic two-dimensional arrays of micromachined microstructures for infrared applications," *Proceedings of the IEEE*, pp.1679-1698, Aug. 1998.

[8] R. Schaumann, "Continuous-time integrated filters-A tutorial," *IEE Proceedings*, pp.184-190, Aug. 1989.